Effective pore radius of the gramicidin channel

Electrostatic energies of ions calculated by a three-dielectric model

Hiroshi Monoi
Department of Physiology, Tohoku University School of Medicine, Sendai, Japan 980

ABSTRACT Electrostatic calculation of the gramicidin channel is performed on the basis of a three-dielectric model in which the peptide backbone of the channel is added as a third dielectric region to the conventional two-dielectric channel model (whose pore radius is often referred to as the effective pore radius r_{eff}). A basic principle for calculating electrostatic fields in three-dielectric models is introduced. It is shown that the gramicidin channel has no unique value of r_{eff}. The r_{eff} with respect to the "self-image energy" (i.e., the image energy in the presence of a single ion) is 2.6–2.7 Å, slightly depending upon the position of the ion (the least-square value over the whole length of the pore is 2.6 Å). In contrast, the r_{eff} with respect to the electric potential due to an ion (and hence the r_{eff} with respect to the interaction energy between two ions) is dependent upon the distance s of separation; it ranges from 2.6 to >5 Å, increasing with an increase in s. However, for the purpose of rough estimation, the r_{eff} with respect to the self-image energy can also be used in calculating the electric potential and the interaction energy, because the error introduced by this approximation is an overestimation of the order of 30% at most. It is also shown that the apparent dielectric constant for the interaction between two charges depends markedly upon the positions of the charges. In the course of this study, the dielectric constant and polarizability of the peptide backbone in the β-sheet structure is estimated to be 10 and 8.22 Å^3.

INTRODUCTION

Previous electrostatic calculations of ionic interaction in the gramicidin channel have assumed that the gramicidin-membrane system could be treated as consisting of two different dielectrics, i.e., a low-dielectric membrane slab pierced by a pore having a dielectric constant equal to that of the aqueous solution outside (Levitt, 1978; Jordan, 1982; Monoi, 1982, 1983).

In this two-dielectric model of the gramicidin channel, the effect of the channel wall (~3 Å in thickness) composed of the polypeptide backbone was approximated by a hypothetical pore whose radius (effective pore radius,[1] r_{eff}) is greater than the physical radius of the pore (~2 Å). Different values have been adopted for r_{eff} by different investigators; 3 Å (Levitt, 1978), 2.4–2.6 Å (Jordan, 1983), 2.5–3.5 Å (Monoi, 1982, 1983). Because those values have no sound theoretical basis (see a later section) and because the image potential is very sensitive to the assigned value of r_{eff} (see, e.g., Fig. 4 *b* in this paper), I feel that it is important to examine this point for further study.

In this work, electrostatic calculation is performed for the three-dielectric model in which the peptide backbone of gramicidin is added as a third dielectric region between the more polarizable pore region and the less polarizable membrane space, and results of calculation are compared with those estimated by the two-dielectric model. For this purpose, a basic principle for the numerical calculation of electric potentials in three-dielectric models is introduced. Ions are supposed to be on the longitudinal axis of the pore.

Conclusions are as follows. In an infinitely long pore with a gramicidin-like cross-section, the effective pore radius r_{eff} is 2.8 Å when the electrostatic energy in the presence of a single ion ("self-image energy") is to be computed. In contrast, the r_{eff} with respect to the interaction energy between two ions is dependent upon the distance s of separation between the ions; it takes a value of 2.8 Å or more, increasing with an increase in distance s. In the gramicidin channel, the r_{eff} with respect to the self-image energy is 2.6–2.7 Å; it depends upon the position of the ion only slightly (its least-square value over the whole length of the pore is 2.6 Å). In contrast, the r_{eff} with respect to the electric field due to an ion (and hence the r_{eff} with respect to the interaction energy between two ions) is dependent on the distance s of separation; it ranges from 2.6 to more than 5 Å, increasing with an increase in s. Thus, the channel has

This work constitutes a part of the manuscript that was presented at the 21st Jerusalem Symposium on Quantum Chemistry and Biochemistry held in Jerusalem, Israel, May 16–19, 1988, which I was invited to by Drs. A. Pullman, J. Jortner, and B. Pullman but could not attend because of my physical condition.

[1]The term "effective pore radius" has been used to imply that when the radius r' of the hypothetical pore in the two-dielectric model is equal to this radius r_{eff}, electric potentials and fields within the pore are equal to those calculated on the basis of the three-dielectric model (cf. Fig. 1).

0006-3495/91/04/786/09 $2.00

no unique value of r_{eff}. For the purpose of a rough estimation, however, the value (2.6 Å) for the r_{eff} with respect to the self-image energy can also be used in computing the electric potential and interaction energy. The error introduced by this approximation is an overestimation of the order of 30% at most.

Relevance of the present estimates of r_{eff} to previously reported values is discussed. It is also reported that the apparent dielectric constant for the interaction between two charges is remarkably dependent upon the position of the charges. In the course of this study, the dielectric constant and polarizability of the peptide backbone in the β-sheet structure are estimated (Appendix).

METHODS

Channel models

Continuum dielectric models are used. Fig. 1 *a* represents a three-dielectric model of the gramicidin channel incorporated into a lipid membrane. A cylindrical pore penetrates a planar membrane of dielectric constant ϵ_3, which is bounded on two sides by semiinfinite aqueous spaces of dielectric constant ϵ_1. The radius r_1 of the pore is taken to be 2.1 Å, and the length l, 27 Å (approximate distance between the average Van der Waals surfaces of the pore ends) on the basis of atomic coordinates of gramicidin A in the single-stranded β-helical form (Koeppe II and Kimura, 1984). The wall of the pore is composed of the β-helical peptide backbone of a gramicidin dimer (Urry et al., 1971; Bamberg et al., 1977; Bradley et al., 1978; Weinstein et al., 1979, 1980; Boni et al., 1986). This region is supposed to be a hollow cylinder of 2.8 Å in thickness (hence, its outer radius r_2 being 4.9 Å) and have a dielectric constant of ϵ_2. This channel model is used in the present study unless otherwise stated.

Fig. 1 *b* depicts a conventional two-dielectric channel model, for which calculation is performed for comparison. In this model, the channel wall (space ϵ_2) is replaced by a hypothetical pore having a radius of r'.

When the thickness of the membrane is greater than the length of the pore, a deformation, or dimpling, of the membrane surface is required to expose the entrance of the pore. The shape of the dimpling around the channel end has recently been calculated (Helfrich and Jakobsson, 1990). The present computation is made only for the case in which the membrane width is equal to the pore length l so that no appreciable dimplings are present at the channel entrances.

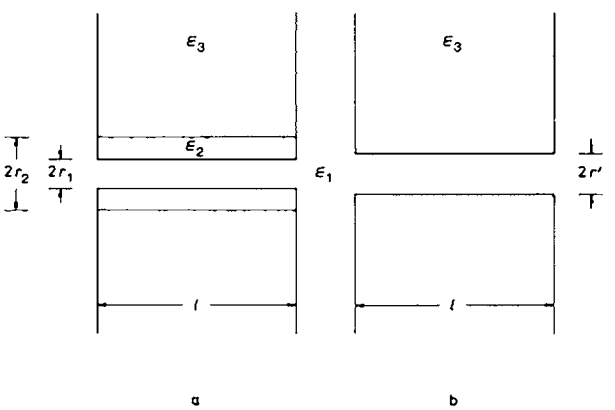

FIGURE 1 Two types of simplified dielectric models of the gramicidin channel. (*a*) Three-dielectric model. (*b*) Two-dielectric model.

The values of dielectric constants ϵ used are: $\epsilon_3 = 2$ (ϵ of saturated hydrocarbons) and $\epsilon_1 = 78$ (a bulk ϵ value of water); unless otherwise stated, $\epsilon_2 = 10$ (see Appendix). The ϵ of the space within the pore has been taken to be equal to ϵ_1 in the precedent works (e.g., Parsegian, 1969; Levitt, 1978; Jordan, 1982; Monoi, 1982) in this field. I follow this treatment. It is assumed that no true charges nor dipoles exist on the surface of, and within, spaces ϵ_2 and ϵ_3.

The ion is treated as a point ion and is placed on the longitudinal axis of the pore. The whole system is cylindrically symmetrical about the pore axis, which is taken as the z-axis of the cylindrical coordinate system; the ρ-coordinate is the distance from the z-axis. The origin of the coordinates is put at the center of the pore. The distance is expressed in angstroms throughout this manuscript.

As a part of the present work, electrostatic calculation was also performed for an infinitely long pore with a gramicidinlike cross-section ($r_1 = 2.1$ Å, $r_2 = 4.9$ Å; $\epsilon_1 = 78$, $\epsilon_2 = 10$, $\epsilon_3 = 2$).

Electrostatic calculation

Electrostatic calculation was performed by the substitute charge method (Ersatzladungsmethode), which was originally developed by Steinbigler (1969). The general principle of this method has been described in a previous paper (Monoi, 1983) and hence is summarized here only briefly.

In this method, continuously distributed electric charges induced on the boundaries between different dielectrics are displaced by a finite number of discrete fictitious charges with appropriate geometries (usually point-, line-, or ring-shaped charges). The fictitious charges are put outside the space where electric potentials and fields are to be calculated. In calculating potentials and fields in space i, it is usually assumed that all other spaces also have the same dielectric constant as that of space i. The number, the locations, and the magnitudes of the fictitious charges are determined so that given boundary conditions can be satisfied exactly at a finite number of points on the boundaries (contour points) and can be satisfied approximately (within a given error) at points on the boundaries other than contour points. Once these parameters are determined, potentials and fields due to the induced surface charges can be obtained as the (vectorial) sum of the potentials and fields due to all the fictitious charges concerned.

Numerical computation was performed with a double (~ 16-figure) precision on a SX-2N supercomputer (NEC Corp., Tokyo, Japan) at the Computer Center of Tohoku University.

Arrangements of fictitious charges and contour points

One of the most important steps in electrostatic calculation by the substitute charge method is to find an optimal arrangement of fictitious charges and contour points. Errors of calculations depend on the arrangement employed.

Fig. 2 represents a main portion of a good arrangement, which was used for the three-dielectric channel model (Fig. 1 *a*) throughout this study. In this arrangement, 532–580 contour points are placed on the boundaries over the range of ρ up to 200–260 Å, depending on the position of true charges. The same number of ring fictitious charges, coaxial with respect to the pore axis (z-axis), are arranged on each side of the boundaries. Those ring charges can be divided into four groups, first two groups, J_1 and J_4, are both placed along by the ϵ_1-ϵ_2 and ϵ_1-ϵ_3 boundaries; J_1 is outside the space ϵ_1, and J_4, inside the space ϵ_1 (Fig. 2

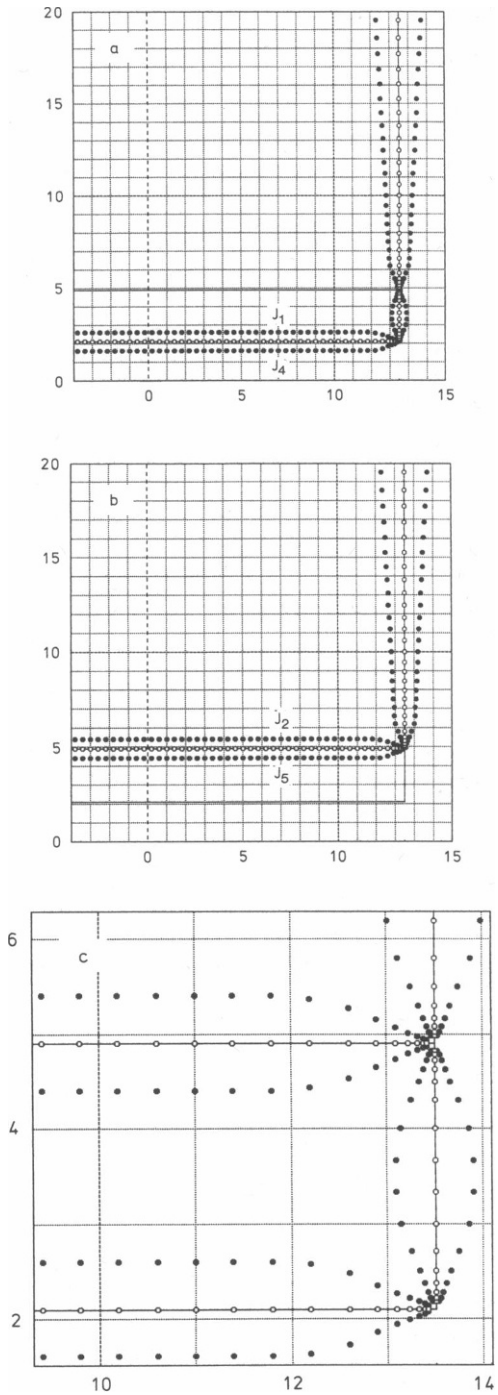

FIGURE 2 An arrangement of fictitious charges and contour points for the three-dielectric channel model. The abscissa and the ordinate represent z- and ρ-coordinates, respectively, expressed in Å. Open circles represent contour points on the boundary, and closed circles, the cross-sections of ring fictitious charges coaxial with respect to the z-axis. (*a* and *b*) Fictitious charges J_1 and J_4 and fictitious charges J_2 and J_5, respectively, and the corresponding contour points (shown only for $\rho \leq 20$ Å and $z \geq -4$ Å). (*c*) Arrangement in the vicinity of the pore entrance. For details, see text.

a). The other two groups, J_2 and J_5, are both positioned along by the ϵ_2-ϵ_3 and ϵ_1-ϵ_3 boundaries; J_2 is inside the space ϵ_3, and J_5, outside the space ϵ_3 (Fig. 2 *b*). The arrangement is cylindrically symmetrical about the pore axis, and is also symmetrical about the center of the pore.

The arrangement used for the two-dielectric channel model (Fig. 1 *b*) is identical with that used for the three-dielectric model, except that the former involves only charges J_2 and J_5 (or only charges J_1 and J_4, which were used when the magnitudes of errors in the boundary conditions were compared between the two species of models) and the corresponding contour points, and except that their ρ-coordinates are altered depending on r'.

In the above channel models, singular points appear at the rectangular phase boundaries at the channel ends. Near those points, the errors in the boundary conditions are very large. To minimize the errors of calculated potentials and fields due to the presence of the singular points, contour points are placed densely near those points up to a distance of 0.08 Å from them (see Fig. 2 *c*). A careful examination implies that the errors of calculated energies do not greatly exceed 0.1% when a true point charge is on the pore axis (also see Monoi, 1983). On the other hand, the error of electric fields was found to be large in the vicinity of the rectangular corners at the pore ends (see the next section and Fig. 3 *b*).

For infinitely long pores, 601 contour points were placed on a phase boundary at an interval of 1 Å. The same number of ring fictitious charges were put on each side of a phase boundary coaxially with respect to the pore axis.

A basic principle for calculating electrostatic fields in three-dielectric models

The boundary conditions at the boundary between spaces of dielectric constants ϵ_i and ϵ_j are

$$\phi_i = \phi_j, \quad D_{in} = D_{jn}, \tag{1}$$

where ϕ_i is the electric potential ϕ in space ϵ_i, and D_{in} is the normal component of the electric displacement D in space ϵ_i on the boundary. When these relations are simply applied for all the ϵ_i-ϵ_j boundaries of the three-dielectric channel model (Fig. 1 *a*), the simultaneous-equation system whose unknowns are the magnitudes of the fictitious charges becomes ill-conditioned so that one cannot get the solution of the equation system. A device for overcoming this difficulty is to employ the following relations as the boundary conditions on the ϵ_1-ϵ_3 boundary:

$$\phi_1 = \phi_2, \quad D_{1n} = D_{2n}, \tag{2}$$

$$\phi_2 = \phi_3, \quad D_{2n} = D_{3n}, \tag{3}$$

and to use fictitious charges J_1 and J_2 in calculating ϕ and D in space ϵ_1; in calculating them in space ϵ_2 and space ϵ_3, charges J_2 and J_4 and charges J_4 and J_5, respectively, are to be used (cf. Fig. 2). This treatment means that *the* ϵ_1-ϵ_3 *boundary is regarded to be both a* ϵ_1-ϵ_2 boundary and a ϵ_2-ϵ_3 *boundary* (assumption of dual character of the ϵ_1-ϵ_3 interface).[2]

[2]An alternative way is to regard the ϵ_2-ϵ_3 boundary to be both a ϵ_1-ϵ_2 and a ϵ_2-ϵ_3 boundary. This treatment saves the computer expenses considerably. In the present work, however, the dual character is supposed for the ϵ_1-ϵ_3 boundary. This is because the magnitudes of the errors in the boundary conditions in the two types of channel models can be compared more appropriately.

The theoretical basis of this treatment is not given here. It will suffice to show that (*a*) if Eqs. 2 and 3 hold true for the ϵ_1-ϵ_3 boundary, then Eq. 1 is also true for this boundary and (*b*) the errors in the boundary conditions are small and/or comparable to those that are calculated for the two-dielectric model by applying the corresponding type of arrangement of fictitious charges and contour points (cf. Methods). The first point is self-evident. The second point is shown below.

The errors in the boundary conditions on the ϵ_i-ϵ_j boundary will be defined by

$$\delta_\phi = (\phi_i - \phi_j)/2, \tag{4}$$

$$\delta_D = (D_{in} - D_{jn})/2, \tag{5}$$

and the relative errors in the boundary conditions, by

$$\delta_\phi^{rel} = (\phi_i - \phi_j)/(\phi_i + \phi_j), \tag{6}$$

$$\delta_D^{rel} = (D_{in} - D_{jn})/(D_{in} + D_{jn}). \tag{7}$$

Fig. 3, *a* and *b*, represent δ_ϕ^{rel} and δ_D^{rel}, respectively, in the three-dielectric model when a true point ion is at the center of the pore. Corresponding errors for the two-dielectric model are also shown for comparison (Fig. 3, *a'* and *b'*). They are plotted only for the portion of the ϵ_1-ϵ_2 boundary facing the pore space. (The magnitudes of relative errors for the ϵ_2-ϵ_3 and ϵ_1-ϵ_3 boundaries and for the remaining portion of the ϵ_1-ϵ_2 boundary are comparable to, or less than, those for the depicted portion of the ϵ_1-ϵ_2 boundary.) The errors were evaluated at three inspection points placed on the boundary with equal spacings between each adjacent contour points (and between a singular point and a nearest-neighbor contour point). In this figure are plotted, for avoiding complication, only the greatest of the relative errors that were found between each two adjacent contour points (and between the singular point and the nearest-neighbor contour point).

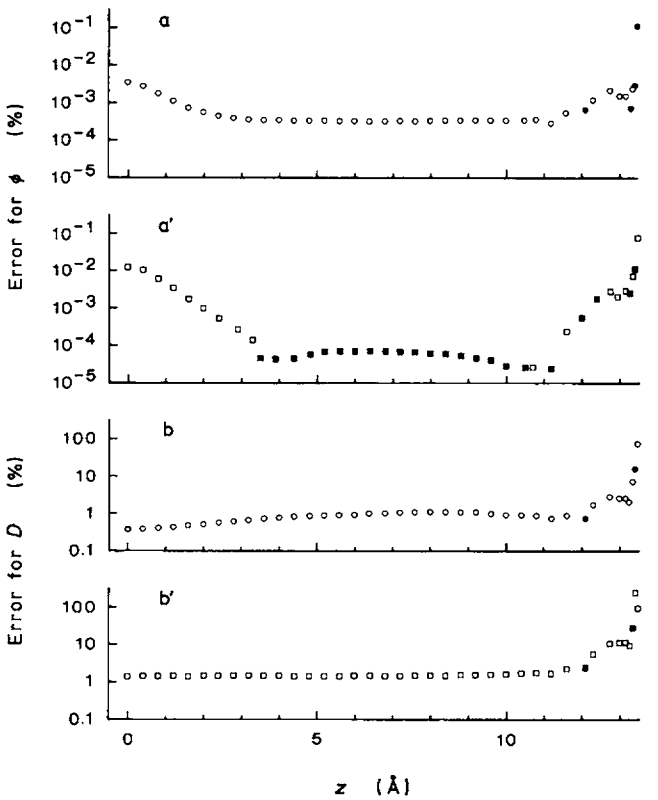

FIGURE 3 Errors in the boundary conditions for the three-dielectric model (*a* and *b*) and the two-dielectric model (*a'* and *b'*). (*a* and *a'*) Relative errors for electric potential ϕ; (*b* and *b'*) relative errors for electric displacement D. A true point charge is supposed to be at the center (z = 0 Å) of the channel. Errors are shown only for the portion of the ϵ_1-ϵ_2 boundary that faces the pore cavity. Only the largest of each set of three errors calculated for three inspection points which are placed, with equal spacings, between each two adjacent contour points (and between the singular point and the nearest-neighbor contour point). Closed circles and squares denote that $\phi_1 > \phi_2$ and $D_{1n} > D_{2n}$, respectively (the vector normal is directed from space ϵ_2 to space ϵ_1).

Fig. 3 *a* indicates that δ_ϕ^{rel} in the three-dielectric model is sufficiently small. It is <0.0035% except for the vicinity of the singular point, where it reaches a maximum but is still in low levels (~0.1% at most). This result is satisfactory.

The case is quite different, however, for δ_D^{rel}. As shown in Fig. 3 *b*, δ_D^{rel} in the three-dielectric model is as large as ~0.4% even near the center of the pore; in the vicinity of the singular points, it reaches up to ~100%.[3] Nevertheless, these values are comparable to the corresponding values of δ_D^{rel} in the two-dielectric model (Fig. 3 *b'*).

As noted in a previous section (section entitled Arrangements of fictitious charges and contour points), singular points appear at the rectangular phase boundaries at channel ends. Large values of δ_D^{rel} in both models are attributable, at least in part, to the occurrence of the singular points, because δ_D^{rel} reduces considerably when the rectangular edges are replaced by smooth surfaces whose geometry is a quarter circle in a plane containing the pore axis (errors in the boundary conditions in the reformed version of the two-dielectric model has been reported in a previous paper; see pp. 77–79 in Monoi, 1983).

RESULTS AND DISCUSSION

Self image energy $\hat{E}_{self}$ and image interaction energy $\hat{E}_{int}$

Before we proceed further, let us define the terms, self image energy and image interaction energy. They are useful for describing the solutions of dielectric problems involving more than one true charge.

When true charges are present in a system composed of spaces having different dielectric constants, surface charges are induced on the boundaries. As electrostatic fields are described by the Poisson equation, the surface charge induced at any point in the presence of more than one true charge is the sum of the surface charges in the presence of each of the true charges. In other words, the surface charges induced by a true charge is independent of the quantities and positions of other true charges, and thus will tentatively be referred to as the "adjoint surface charge" of the true charge.

The potential energy of a true charge due to its adjoint

[3] As easily seen from Eq. 7, a value of $|\delta_D^{rel}|$ close to 100% means that $|D_{1n}| \gg |D_{2n}|$ or $|D_{1n}| \ll |D_{2n}|$; a value of $|\delta_D^{rel}|$ greater than 100% signifies that D_{1n} and D_{2n} are opposite in sign.

surface charge will be named "self image energy" and designated by $\hat{E}_{self}$. The self image energy of a true charge is equal to the potential energy when only the true charge in question is present in the system.

The potential energy, E_{int}, of a true charge due to other true charges involves two contributions, one of which is the Coulomb potential due to other true charges when all the spaces are supposed to have the same dielectric constant as that of the space where the true charge in question is present. This contribution is denoted by E^0_{int}. The other is the potential energy due to the adjoint surface charges of other true charges. It will be called "image interaction energy" (or "image component" of the interaction energy) and represented by $\hat{E}_{int}$. We have

$$E_{int} = E^0_{int} + \hat{E}_{int}. \quad (8)$$

The total electrostatic energy E of a true charge is the sum of $\hat{E}_{self}$ and E_{int}.

Similarly, the electric potential due to the adjoint surface charges will be called the "image component" of electric potential ϕ and denoted by ϕ_{image}.

Obviously, $\hat{E}_{self}$ of a true charge is independent of other true charges, and ϕ_{image} (and hence ϕ) due to a true charge is also independent of other true charges; $\hat{E}_{int}$ (and hence E_{int}) of a true charge due to a second true charge is independent of true charges other than the two true charges in question. In general, $\hat{E}_{int}$ (and ϕ_{image}) due to a true charge is not inversely proportional to the distance from the true charge, as will be seen later.

Effective pore radius with respect to the self image energy; profile of self image energy

Fig. 4 *a* shows the dependence of the potential energy E of a monovalent point ion upon ϵ_2 in the three-dielectric model (Fig. 1 *a*) of the gramicidin channel. Fig. 4 *b* expresses the dependence of E of a monovalent point ion upon the hypothetical pore radius r' in the two-dielectric model (Fig. 1 *b*). As in Fig. 4 *b*, E is very sensitive to the variation of r'; when r' varies from 2.5 to 3.5 Å, E decreases from 5.83 to 3.23 kcal/mol (a 45% decrease) when the ion is at the center of the pore.

A value of 10 can be ascribed to ϵ_2 (see Appendix). By comparing data in Fig. 4 *a* and *b*, effective pore radius r_{eff} was found to be 2.66 and 2.59 Å for a single ion positioned at $z = 0$ and at 11.5 Å, respectively. The difference between these values of r_{eff} is small. By least-squares fitting, r_{eff} was computed to be 2.64 Å for the range of z between −18 and +18 Å.

As indicated in Fig. 5, the potential energy profile of a single ion calculated by the three-dielectric model is well

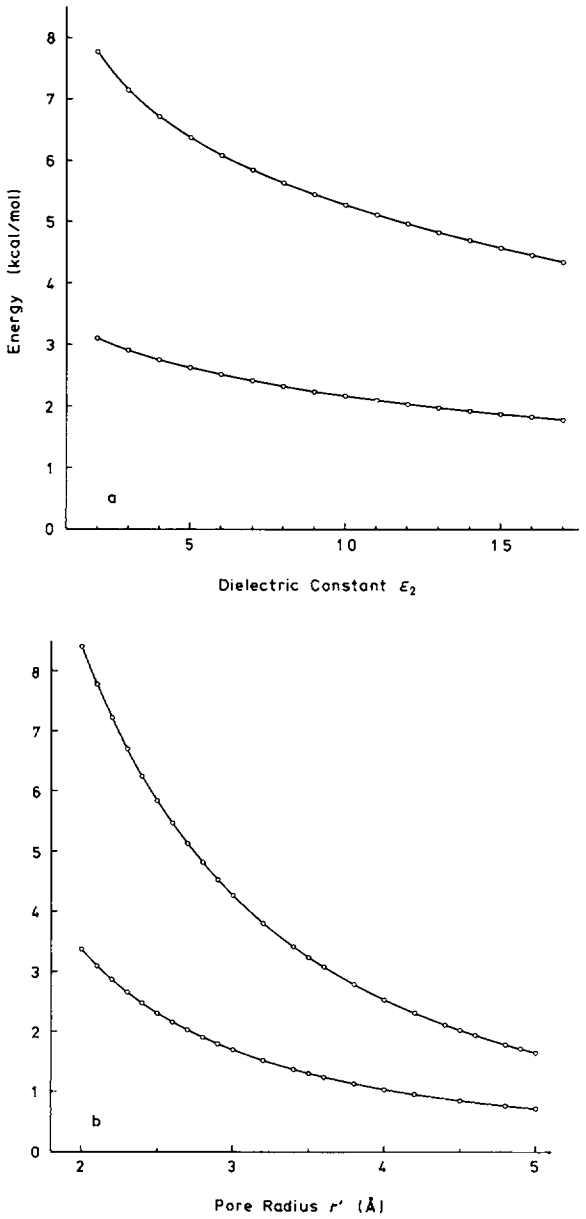

FIGURE 4 Dependence of the potential energy of a monovalent point ion upon (*a*) the dielectric constant ϵ_2 of the channel wall in the three-dielectric model and (*b*) hypothetical pore radius r' in the two-dielectric model. The ion is supposed to be at $z = 0$ Å (*upper curve*) and 11.5 Å (*lower curve*) on the longitudinal axis of the pore. Open circles represent calculated points.

mimicked by the two-dielectric model when this value of r_{eff} is used. Accordingly, the r_{eff} of the gramicidin channel with respect to the potential energy is 2.64 Å when only a single ion is present in the channel.

As stated in the preceding section, the self image energy $\hat{E}_{self}$ of an ion remains the same irrespective of the

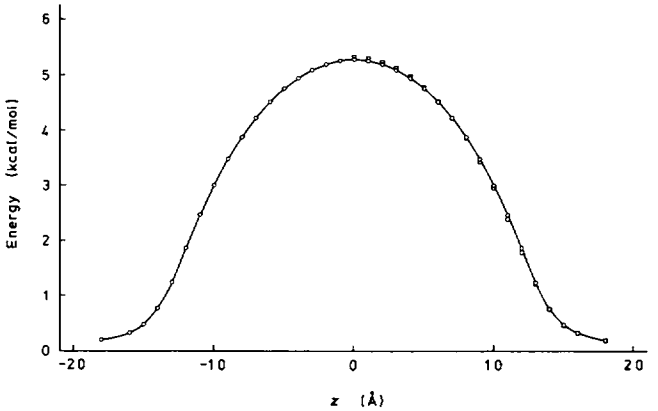

FIGURE 5 Potential energy profile of a monovalent point ion within the gramicidin channel, calculated by the three-dielectric model (*open circles*) and by the two-dielectric model (*open squares;* plotted only for $z \geq 0$ Å). Pore radius r' in the latter model is taken to be 2.64 Å. The ion is on the longitudinal axis of the pore.

presence or absence of other true charges. Therefore, even when more than one ion is present within the channel, the r_{eff} with respect to the self image energy of any ion remains the same irrespective of the other ions. As shown above, it depends upon the position of the ion only slightly, and its least-squares value is 2.64 Å.

Some results of calculation will be added here concerning an infinitely long pore with a gramicidinlike cross-section ($r_1 = 2.1$ Å, $r_2 = 4.9$ Å; $\epsilon_1 = 78$, $\epsilon_2 = 10$, $\epsilon_3 = 2$). A monovalent point ion placed on the pore axis was computed to have a self image energy of 10.03 kcal/mol, in contrast with the value 5.27 kcal/mol for the energy of a monovalent point ion positioned at the center of the gramicidin channel. Thus, the finite length of this channel decreases the image energy by 47%. The effective pore radius r_{eff} (with respect to the self image energy) of this pore was found to be 2.82 Å, in contrast with the corresponding value 2.66 Å for an ion placed at the center of the gramicidin channel. Thus, a finite length of pore decreases the effective pore radius r_{eff}.

Effective pore radius with respect to the electric potential and the interaction energy

In contrast with the r_{eff} with respect to the self image energy $\hat{E}_{self}$, the r_{eff} with respect to the electric potential ϕ due to an ion was found to possess no unique value; it depends on the distance s from the ion. It ranges from 2.6 to >5 Å, increasing with an increase in s. Table 1 illustrates this situation. In this table, a point ion is supposed to be at $z = 12$ Å, and ϕ and its image component ϕ_{image} due to the ion are given for three levels

TABLE 1 **Electric potentials ϕ due to an ion calculated by the three- and the two-dielectric model**

z		Electric Potential* 3-dielectric model	Electric Potential* 2-dielectric model‡		r_{eff}§
Å		*volts*	*volts*		Å
12.0	(ϕ_{image})	0.1610	0.1556	(0.97)	2.59
	(ϕ)	∞	∞		—
0.0	(ϕ_{image})	0.0962	0.1141	(1.19)	3.1
	(ϕ)	0.1115	0.1295	(1.16)	
−12.0	(ϕ_{image})	0.0151	0.0211	(1.40)	5.1
	(ϕ)	0.0228	0.0288	(1.26)	

A monovalent point ion is placed at $z = 12$ Å on the longitudinal axis of the pore. *Electric potential on the pore axis at z indicated, due to the ion. ‡Pore radius r' is taken to be 2.64 Å, which is the r_{eff} with respect to the self image energy $\hat{E}_{self}$. The figures in the parentheses represent the ratio of the electric potential in the two-dielectric model (the fourth column) to that in the three-dielectric model (the third column). §The r_{eff} with respect to the electric potential, i.e., the value of pore radius r' in the two-dielectric model that gives the same magnitude of electric potential as that in the three-dielectric model.

of s (= 0, 12, and 24 Å). The corresponding values for the r_{eff} with respect to ϕ (and hence to ϕ_{image}) are listed in the last column. For $s = 0$ Å ($z = 12$ Å), the r_{eff} with respect to ϕ is 2.6 Å; it increases up to 3.1 and 5.1 Å for $s = 12$ and 24 Å ($z = 0$ and -12 Å), respectively. The r_{eff} with respect to ϕ due to an ion also depends upon the position of the ion, but in a less extent (data not shown).

Therefore, the r_{eff} with respect to the interaction energy E_{int} between two ions also increases with the distance s between them. It ranges from 2.6 to >5 Å.

As a consequence, if one uses the r_{eff} with respect to the self image energy (= 2.64 Å) in computing interaction energies by the two-dielectric model, he may get overestimated values. As illustrated in Table 1 (fifth column), the overestimation is of the order of 30 and 40% at most for E_{int} and $\hat{E}_{int}$, respectively, for two ions situated near the opposite ends of the channel (also see footnote 4 in the next section). For the purpose of rough estimation, therefore, the value (2.64 Å) of the r_{eff} with respect to the self image energy can also be used in calculating the interaction energy.

In an infinitely long pore with a gramicidinlike cross-section, the r_{eff} with respect to the interaction energy between two ions was 2.82 Å or more, increasing with the distance s of separation.

It is also noted that the image component ϕ_{image} of the electric potential ϕ (and hence ϕ itself and the interaction energy E_{int}) due to a point charge is not inversely proportional to the distance from the charge. This will immediately be seen from Table 1 (third column). In this

table, potential ϕ at $z = -12$ Å due to a charge placed at $z = 12$ Å is ~1/5 of ϕ at $z = 0$ Å, in spite of the fact that the distance from the charge increases by a factor of two. This observation implies that the apparent dielectric constant for the interaction between two charges is markedly dependent on the positions of the charges (also see a later section entitled Apparent dielectric constants).

Several values of the self image energy and the interaction energy

Table 2 lists several values of the self image energy $\hat{E}_{self}$ and the interaction energy E_{int} calculated by the three-dielectric model. As shown in this table, $\hat{E}_{self}$ of a monovalent point ion positioned at the center of the channel is 5.27 kcal/mol. The cation binding site with highest affinity is known to be located near both ends of the channel. Reported values for the exact position of the binding site vary depending on the species of ions and the investigators, ranging between 10.5 and 12.5 Å from the center of the channel (Koeppe II et al., 1979; Andersen, 1981; Etchebest et al., 1985; Etchebest and Pullman, 1986, 1988; Jordan, 1987). At those possible positions of the cation binding sites ($z = \pm 10.5 - \pm 12.5$ Å), $\hat{E}_{self}$ is 2.7–1.5 kcal/mol for a monovalent point ion.

Table 2 also involves interaction energies E_{int} between two monovalent point cations situated near the opposite ends of the channel. For the possible positions of the cation binding sites ($z = \pm 10.5 - \pm 12.5$ Å), E_{int} is 1.02–0.41 kcal/mol. This means that the ratio of the binding constants for the binding of the first and the second cation (K_1/K_2) is 5.6–2.0 if the interaction between the channel and a bound cation remains unvaried irrespective of the presence or absence of another cation at the opposite end.[4]

Apparently, $\hat{E}_{self}$ and E_{int} for divalent ions are four times those for a monovalent ion. The values for image energies and for the ratio K_1/K_2 given above are for the channel incorporated into a thin membrane having no appreciable dimplings at the channel entrances. In the presence of the dimplings, they are expected to increase, especially the ratio K_1/K_2 (cf. Table 2 in Monoi, 1983).

TABLE 2 **Self image energy $\hat{E}_{self}$ and interaction energy E_{int} in the gramicidin channel**

Ion occupancy	Position of ions*	$\hat{E}_{self}$	$\hat{E}_{int}$	E_{int}	K_1/K_2
	Å		*kcal/mol*		
Single	0.0	5.27	—	—	—
	10.5	2.74	—	—	—
	11.5	2.16	—	—	—
	12.5	1.54	—	—	—
Double‡	±10.5	5.47	0.819	1.022	5.6
	±11.5	4.32	0.482	0.667	3.1
	±12.5	3.09	0.237	0.407	2.0

Point monovalent ions are supposed to be on the longitudinal axis of the pore. Energies are calculated by the three-dielectric model. Self image energy $\hat{E}_{self}$ for the double occupancy is the sum of $\hat{E}_{self}$ of the two ions. *Measured from the center of the pore. ‡Ionic charges are of the same sign.

TABLE 3 **Apparent dielectric constant ϵ_{app} in the gramicidin channel**

Position of ions*	Distance	ϵ_{app}
Å	Å	
±5.0	10.0	6.61
±7.5	15.0	8.15
±10.0	20.0	13.4
±10.5	21.0	15.5
±12.5	25.0	32.6
±14.0	28.0	65.2
5.0, 15.0	10.0	20.8

Two point ions are supposed to be on the longitudinal axis of the pore. The apparent dielectric constant ϵ_{app} is calculated as $(E_{int})_{vac}/E_{int}$, where E_{int} is the interaction energy between the two ions, and $(E_{int})_{vac}$ is E_{int} in vacuum. Energies are calculated by the three-dielectric model. *Measured from the center of the pore.

Apparent dielectric constants

Table 3 presents the apparent dielectric constant ϵ_{app} for the interaction energy E_{int} between two point ions placed on the pore axis. It is 15–33 for two ions located at the possible positions of the cation binding sites ($z = \pm 10.5 - \pm 12.5$ Å). It decreases to <7 for two ions separated by 10 Å near the center of the pore ($z = \pm 5$ Å). It is noteworthy that this value for ϵ_{app} is less than the dielectric constant of the polypeptide backbone comprising the channel wall ($\epsilon = 10$). The apparent dielectric constant is thus remarkably dependent on the positions of ions concerned.

Relevance to previous values for the self image energy and the effective pore radius

Gramicidin channel

Levitt (1978) and Monoi (1982, 1983) used the values 3 and 2.5–3.5 Å, respectively, for effective pore radius r_{eff}

[4]If one uses the r_{eff} with respect to the self-image energy (= 2.64 Å) to calculate interaction energies by means of the two-dielectric model (Fig. 1 *b*), the estimates of E_{int} and K_1/K_2 increase to 1.25–0.52 kcal/mol and 8.2–2.4, respectively, for the possible positions of the cation binding sites ($z = \pm 10.5 - \pm 12.5$ Å).

of the gramicidin channel. These values are based on no explicit theories.

According to Jordan (1981, 1983), (*a*) the electrostatic energy of a monovalent point ion positioned at the center of the gramicidin channel ($E_s(L)$ in his notation) is in the range of 24.6–28.1 kJ/mol (5.88–6.71 kcal/mol), and hence (*b*) effective pore radius r_{eff} is in the range of 2.4–2.6 Å. These estimates resemble the corresponding values obtained in the present work (5.27 kcal/mol and 2.7 Å, respectively). Jordan's estimates, however, were calculated on different bases. A brief comment is added below on his estimation of image energies and r_{eff}.

His estimation is based on the following relation (Eq. 13 in Jordan, 1981)

$$\epsilon_2 f + \epsilon_3(1 - f) = \epsilon_{PF}, \tag{9}$$

where ϵ_2 and ϵ_3 have the same meanings as in the present manuscript; i.e., ϵ_2 is the dielectric constant ϵ of the peptide backbone of the channel, and ϵ_3 is ϵ of the membrane (~ 2). Parameter ϵ_{PF} is ϵ of the pore former, or gramicidin (~ 4), and f means the volume fraction of the peptide backbone in gramicidin. Parameter f was taken to be 0.36, and hence ϵ_2 is 7.6 when calculated from Eq. 9.

Unfortunately, Eq. 9 is not applicable to this case because this type of equation can be used only when the difference between ϵ_2 and ϵ_3 is small. A more appropriate equation for the dielectric constant of a mixture of dielectrics is

$$\frac{\epsilon_m - 1}{\epsilon_m + 2} = \sum_k f_k \frac{\epsilon_k - 1}{\epsilon_k + 2}, \tag{10}$$

where ϵ_m is dielectric constant ϵ of the mixture, and ϵ_k is ϵ of the kth component; f_k means the volume fraction of the kth component. Eq. 10 can be derived from the Clausius-Mossotti equation (e.g., Böttcher, 1973).

Let us adopt the same line of calculation and the same values of parameters as employed by Jordan (1981, 1983), except that Eq. 10 is applied instead of Eq. 9. Then, ϵ_2 is 52 from Eq. 10, and (*a*) $E_s(L)$ is in the range of 10.5–19.5 kJ/mol (2.51–4.66 kcal/mol), and hence (*b*) r_{eff} is in the range of 3.0–4.2 Å. These values are very different from the present estimates.

In his calculation, Jordan (1981) supposed the polar region of the gramicidin to be in a thickness of 2 Å, which are evidently too small when the Van der Waals radii of the C, N, and O atoms are considered. A smaller thickness of the polar region leads to a greater value of ϵ and hence to smaller image energies and a greater r_{eff}, whereas, as shown above, the application of Eq. 9 leads to a smaller value of ϵ and hence to greater image energies and a smaller r_{eff}.

That is to say, the application of Eq. 9 and the use of a smaller thickness (2 Å) of the polar region have opposite effects upon the estimates of image energies and r_{eff}. Moreover, the opposite effects are similar in magnitude to each other in this case. This is the reason why Jordan's estimates of image energies and of r_{eff} are not far from being proper, in spite of the fact that he applied Eq. 9.

Infinitely long pore

The present calculation also indicates that within an infinitely long pore with a gramicidinlike cross-section, the image energy of a monovalent cation (positioned at the pore axis) is 10.03 kcal/mol, and that the effective pore radius of this pore is 2.82 Å. Corresponding values reported by Jordan are 46.1 or 11.0 kcal/mol (Jordan, 1981) and 2.5 Å (Jordan, 1984), respectively, which were estimated by supposing Eq. 9 and a 2 Å thickness of the polar region (polypeptide backbone) of the gramicidin channel.

APPENDIX

Dielectric constant and polarizability of polypeptide backbone in the β-sheet structure

Tredgold and Hole (1976) measured the dielectric constant ϵ of dry synthetic polyalanylglycine (PAG) film in the antiparallel β-sheet structure, a structure similar to that of the gramicidin channel. The value of ϵ of this film was four for lower frequencies at physiological temperatures.

The whole space occupied by this PAG film can be regarded as comprised of two types of minor spaces, each of which is a planar slab in geometry and interposes between two slabs of the other type. One of the two types (space A) is comprised of the peptide backbone, and the other (space B) involves alanyl (CH_3—) and glycyl (H—) side groups of the polypeptide. The thickness of space A is taken to be 2.8 Å. Together with the value 9.7 Å for the interplanar spacing of the crystal structure of the PAG film (Tredgold and Hole, 1976), the thickness of space B is 2.05 Å, and volume fractions, f_A and f_B, of spaces A and B are 0.58 (= 2.8/4.85) and 0.42 (= 2.05/4.85), respectively (interplanar spacing involves two sheets of polypeptides).

The dielectric constant, ϵ_B, of space B can be calculated from the bond polarizabilities, α_{C-H} and α_{C-C}, of the C—H and C—C bonds: $\alpha_{C-H} = 0.655$ Å^3/bond and $\alpha_{C-C} = 0.475$ Å^3/bond (taken from Webb, 1963). The polarizability α of an alanyl side group is hence 2.203 Å^3 ($= 3\alpha_{C-H} + 0.5\alpha_{C-C}$; half of α_{C-C} was assigned to space A). Similarly, α of a glycyl side group is 0.327 Å^3 ($= 0.5\alpha_{C-H}$; half of α_{C-H} was assigned to space A). From the Clausius-Mossotti equation, ϵ_B is given by

$$\frac{\epsilon_B - 1}{\epsilon_B + 2} = \frac{4\pi}{3} N_B \alpha_B, \tag{A1}$$

where α_B is the sum of the polarizabilities of an alanyl and a glycyl side group ($\alpha_B = 2.530$ Å^3), and N_B is half the number of side groups per 1 Å^3 of space B. The interchain spacing of PAG in the β-structure is 4.71 Å, and the axial translation distance per one amino acid residue is 3.48 Å (Frazer et al., 1965). Together with the value of the thickness of

space B given above (2.05 Å), N_B is calculated to be 0.0149 Å^{-3}. Hence ϵ_B is 1.56 from Eq. A1.

On the other hand, the dielectric constant, ϵ_A, of space A is, from Eq. 10,

$$\epsilon_A = \frac{1 + 2p_A}{1 - p_A}, \tag{A2}$$

$$p_A = \frac{p_{PAG} - f_B p_B}{f_A}, \tag{A3}$$

$$p_{PAG} = \frac{\epsilon_{PAG} - 1}{\epsilon_{PAG} + 2}, \tag{A4}$$

where ϵ_{PAG} is the dielectric constant of the PAG film (= 4), and p_B is identical with the left-hand side of Eq. A1. From Eqs. A2–A4, we finally get ϵ_A = 10 as the dielectric constant of the peptide backbone in the β-sheet structure. (If the thickness of space A is inceased [or decreased] by 0.1 Å, then the resultant value of ϵ_A decreases [or increases] by ~ 10%.)

From an equation similar to Eq. A1, the polarizability, α_{PAG}, of the PAG film per one amino acid residue is calculated to be 9.49 Å^3. Thus, the polarizability of the polypeptide backbone in the β-sheet structure is 8.22 Å^3 (= $\alpha_{PAG} - \alpha_B/2$) per residue, which is independent of the assigned value of the thickness of space A.

In the present work, the value ϵ = 10 was used for the dielectric constant of the peptide backbone of the gramicidin channel.

The present work was supported by a Grant-in-Aid for Special Project Research on Molecular Mechanism of Bioelectrical Response (59223004, 60215002, 61107002) from the Japanese Ministry of Education, Science and Culture.

Received for publication 22 June 1990 and in final form 5 November 1990.

REFERENCES

Andersen, O. S., E. W. Barrett, and L. B. Weiss. 1981. On the position of the alkali metal cation binding sites in gramicidin channels. *Biophys. J.* 33:63a. (Abstr.)

Bamberg, E., H. J. Apell, and H. Alpes. 1977. Structure of the gramicidin A channel: discrimination between the $\pi_{L,D}$ and the β helix by electrical measurements with lipid bilayer membranes. *Proc. Natl. Acad. Sci. USA.* 74:2402–2406.

Boni, L. T., A. J. Connolly, and A. M. Kleinfeld. 1986. Transmembrane distribution of gramicidin by tryptophan energy transfer. *Biophys. J.* 49:122–123.

Böttcher, C. J. F. 1973. Theory of Electric Polarization. Vol. 1. Elsevier Scientific Publishing Co., Amsterdam. 377 pp.

Bradley, R. J., D. W. Urry, K. Okamoto, and R. Rapaka. 1978. Channel structures of gramicidin: characterization of succinyl derivatives. *Science (Wash. DC).* 200:435–437.

Etchebest, C., and A. Pullman. 1986. The gramicidin A channel: energetics and structural characteristics of the progression of a sodium ion in the presence of water. *J. Biomol. Struct. & Dyn.* 3:805–825.

Etchebest, C., and A. Pullman. 1988. Energy profile of Cs^+ in gramicidin A in the presence of water. Problem of the ion selectivity of the channel. *J. Biomol. Struct. & Dyn.* 5:1111–1125.

Etchebest, C., A. Pullman, and S. Ranganathan. 1985. The gramicidin A channel: theoretical energy profile computed for single occupancy by a divalent cation, Ca^{2+}. *Biochim. Biophys. Acta.* 818:23–30.

Fraser, R. D. B., T. P. MacRae, F. H. C. Stewart, and E. Suzuki. 1965. Poly-L-alanylglycine. *J. Mol. Biol.* 11:706–712.

Helfrich, P., and E. Jakobsson. 1990. Calculation of deformation energies and conformations in lipid membranes containing gramicidin channels. *Biophys. J.* 57:1075–1084.

Jordan, P. C. 1981. Energy barriers for passage of ions through channels. Exact solution of two electrostatic problems. *Biophys. Chem.* 13:203–212.

Jordan, P. C. 1982. Electrostatic modeling of ion pores. I. Energy barriers and electric field profiles. *Biophys. J.* 39:157–164.

Jordan, P. C. 1983. Electrostatic modeling of ion pores. II. Effects attributable to the membrane dipole potential. *Biophys. J.* 41:189–195.

Jordan, P. C. 1984. The total electrostatic potential in a gramicidin channel. *J. Membr. Biol.* 78:91–102.

Jordan, P. C. 1987. Why is gramicidin valence selective? A theoretical study. *Biophys. J.* 51:661–672.

Koeppe II, R. E., and M. Kimura. 1984. Computer building of β-helical polypeptide models. *Biopolymers.* 23:23–38.

Koeppe II, R. E., J. M. Berg, K. O. Hodgson, and L. Stryer. 1979. Gramicidin A crystals contain two cation binding sites per channel. *Nature (Lond.).* 279:723–725.

Levitt, D. G. 1978. Electrostatic calculations for an ion channel. I. Energy and potential profiles and interactions between ions. *Biophys. J.* 22:209–219.

Monoi, H. 1982. Possible existence of ion pairs at the mouths of ion channels. *Biochim. Biophys. Acta.* 693:159–164.

Monoi, H. 1983. Ionic interactions and anion binding in the gramicidin channel. An electrostatic calculation. *J. Theor. Biol.* 102:69–99.

Parsegian, A. 1969. Energy of an ion crossing a low dielectric membrane: solutions to four relevant electrostatic problems. *Nature (Lond.).* 221:844–846.

Steinbigler, H. 1969. Digitale Berechnung elektrischer Felder. *Elektrotechnishe Zeitschrift, Ausgabe A.* 90:663–666.

Tredgold, R. H., and P. N. Hole. 1976. Dielectric behaviour of dry synthetic polypeptides. *Biochim. Biophys. Acta.* 443:137–142.

Urry, D. W., M. C. Goodall, J. D. Glickson, and D. F. Mayers. 1971. The gramicidin A transmembrane channel: characteristics of head-to-head dimerized $\pi_{(L,D)}$ helices. *Proc. Natl. Acad. Sci. USA.* 68:1907–1911.

Webb, J. L. 1963. Enzyme and Metabolic Inhibitors. Vol. 1. Academic Press, New York. 949 pp.

Weinstein, S., B. A. Wallace, E. R. Blout, J. S. Morrow, and W. R. Veatch. 1979. Conformation of gramicidin A channel in phospholipid vesicles: a ^{13}C and ^{19}F nuclear magnetic resonance study. *Proc. Natl. Acad. Sci. USA.* 76:4230–4234.

Weinstein, S., B. A. Wallace, J. S. Morrow, and W. R. Veatch. 1980. Conformation of the gramicidin A transmembrane channel: a ^{13}C nuclear magnetic resonance study of ^{13}C-enriched gramicidin in phosphatidyl choline vesicles. *J. Mol. Biol.* 143:1–19.